Int. J. Electrochem. Sci., 11 **(2016)** 4300 – 4309, doi: 10.20964/2016.06.87

International Journal of ELECTROCHEMICAL SCIENCE
www.electrochemsci.org

Ammonia Oxidation on the Barium Doped Nano Structured PbO_2 Electrode: An Electrochemical Preparation and Application

Karunakaran Kannan, Govindan Muthuraman, and Moon Il- Shik[*]

Department of Chemical Engineering, Sunchon National University, #255 Jungangno, Suncheon 540-742, Jeollanam-do, Republic of Korea.
[*]E-mail: ismoon@sunchon.ac.kr

Received: 8 March 2016 / *Accepted:* 25 April 2016 / *Published:* 4 May 2016

In the present investigation, we report a novel nano structured Ba/PbO_2 prepared by electrochemical deposition method has been employed for the effective oxidation of ammonia in aqueous solutions. The electrode deposition was achieved in the boric acid bath solution that yielded a smooth deposition of PbO_2 without poisoning the supporting electrolyte. The surface characterization of the deposited layer was done using Scanning Electron Microscope (SEM), and observed that cauliflower like morphology of undoped PbO_2 was completely changed to a sharp edge like flower shape morphology due to the addition of Barium ions. The XRD characterization showed that nano crystallinity of PbO_2 gets altered with the concentration of the Barium (Ba) ion dopant. Cyclic voltammetric investigation indicated that $Ba_{10\text{-}5}/PbO_2$ electrode effectively oxidized Ammonia (NH_3) in alkaline solution, as confirmed through FT-IR spectral analyses. The prepared Ba containing electrode layer is quite promising for the oxidization of Ammonia for various industrial applications.

Keywords: Electro-deposition, Nano structure, Barium doped PbO_2, Ammonia oxidation.

1. INTRODUCTION

Ammonia is an essential natural resource for the biological as well as environmental concerns, which exists naturally in the air at levels between 1 and 5 parts in a billion parts of air (ppb). At the same time, if exceeds even slightly elevated concentrations (hyperammonemia) are toxic to the central nervous system (CNS) to the human [1]. So, detection or destruction of ammonia detection is important in the fields of the diagnosis of diseases such as renal inadequacy and diabetes [2,3,4,5] and ammonia levels rise in the blood, more ammonia is leaked into the brain, potentially leading to brain damage, leads to a condition, hepatic encephalopathy, that manifests as sleep disturbances, mood

disorders, poor cognition, anxiety, depression and movement disorders [6]. Also, ammonia determination is important in water samples where it indicates organic material decomposition which can be harmful to human health, whilst higher ammonia levels are of analytical interest in industrial operations such as refrigeration or fertilizer manufacture.

Ammonia oxidation is a slow process at low temperatures and efficient methods are required to convert ammonia to nitrogen at reasonable reaction rates. There are different methods for the oxidation of ammonia such as by thermal degradation [7,8,9], electrochemical oxidation [10], photoelectron catalytic oxidation[11], metal catalyst Pt, Pd, Ir, Ru, Ag [12], and metal oxides like Co_3O_4, MnO_2 or V_2O_5 [13], main group oxides such as SnO_2 [14], and a bimetallic mixed oxides catalyst such as Fe_2O_3-Al_2O_3 [15], ZrO_2/Al_2O_3 [16]. Metal oxides are more effective for ammonia oxidation but need to be operated at higher temperature. The electro-catalytic oxidation methods provide simple and room temperature destruction of ammonia. The well accepted mechanism of ammonia oxidation in alkaline solutions on Pt electrode was proposed by [17] and involves dehydrogenation of adsorbed ammonia and formation of N_2 gas. To over come these problems, we need enough technique for complete degradation of ammonia to N_2 gas. But, adsorption of atomic nitrogen blocks active sites leading to complete Pt deactivation. In the recent past, many electrodes like BDD [18], SnO_2 [19] and IrO_2 [20], have been found more effective oxidation of ammonia. In particular, Lead based alloys and oxide materials on metal substrates like Ti/PbO_2 [21], Ti/SnO_2+Sb/PbO_2 [22], CNT (Carbon nano tube)/PbO_2 [23], Ti/Pt/PbO_2 [24], and PbO_2/CPE [25], electrodes found effective oxidation of NH_3 gas. All above-mentioned works were done using bulk metal or metal oxide electrodes with high precious metal loading, whereas to develop efficient and economically viable electrodes the amount of precious metals must be reduced. This can be achieved by using electrocatalysts in the form of nanoparticles dispersed on high surface area conductive supports. It is well known that ex-situ synthesis of nano-particles ended up less adherence and conductivity problems with the support. Electrochemical in-situ nano particle preparation of bimetallic metal oxides provide not only adherence but also can be control the structure of the nano particles.

In the present work, alkali earth metal barium selected as dopant to nano structured PbO_2 electrode. It is known that alkali earth metal oxide such as MgO [26], BaO [27], have been reported be a property of sensing NO_X, In specifically $BaSO_4/PbO_2$ [28, 29] material have been reported. We believe that addition of Ba^{2+}ion, the PbO_2 catalytic activity and adherence is increased predominantly. Here, we have synthesized nano structured Ba doped PbO_2 by electrochemical method, the optimized Ba. PbO_2 was subjected to oxidized NH_3 at NaOH medium. The composition and morphology were analyzed by the XRD and SEM respectively. Ammonia oxidation property of Ba.PbO_2 was characterized by cyclic voltammetry and FT-IR spectroscopy.

2. MATERIALS AND METHODS

Chemicals and reagents were used for the synthesis of barium doped PbO_2 electrode: $Pb(NO_3)_2$ (99.9%) Kanto Chemical Co.Ltd , H_3BO_3(99%) OCI Company Ltd, $Ba(Ac)_2$ (99%), Ammonia solution (25%-28%) and Na_2SO_4 (99.9%) were purchased from Daejung Chemicals &metals Co.Ltd, Na_2HPO_4

(99%) Duksan Pure Chemicals Co.Ltd, $NaH_2PO_4.2H_2O$ (99.9%) Junsei Chemicals Co.Ltd, were used without further purifications

2.1 Electrode pretreatment

To fabricate the Ba doped PbO_2 (Ba/PbO_2), Titanium electrode of 1x1 cm^2 and Graphite of 1x1 cm^2 was used as anode and cathode respectively. The Ti anode was first sandblasted on SiC paper to improve the surface roughness, followed by sonicated in CH_3CHO to remove all un dissolved wastes. Then Ti electrode put into 40 % NaOH and boil at 80°C for 2 h, followed by washed with 15 % hot oxalic acid solution for 1 h until the solution color changed to black brownish, finally the Ti electrode washed in DI water.

2.2 Preparation of Ba doped PbO_2 electrode

0.3 M of $Pb(NO_3)_2$ mixed with 0.2M of H_3BO_3 in 50 ml DI water, then $Ba(Ac)_2$ concentration as $2x10^{-1}$ M, $2x10^{-3}$ M, $2x10^{-5}$ M, $2x10^{-7}$ M individually prepared and mixed along with above solution and heat at 65°C to get clear solution. Fig. 1. Depicted The schematic diagram of electrochemical cell, where pretreated Ti electrode was used as anode and carbon as cathode, respectively, and separated by the distance of 1cm, and the electrolysis was carried out by passing current density of 5 mA/cm^2 for 10 min. The Thin hard Ba/PbO_2 layer was deposited, and washed in DI water and dry at 120°C for 1 h. Hereafter, Barium ion concentrations will be denoted as $Ba_{10\text{-}1}/PbO_2$, $Ba_{10\text{-}3}/PbO_2$, $Ba_{10\text{-}5}/PbO_2$, $Ba_{10\text{-}7}/PbO_2$.

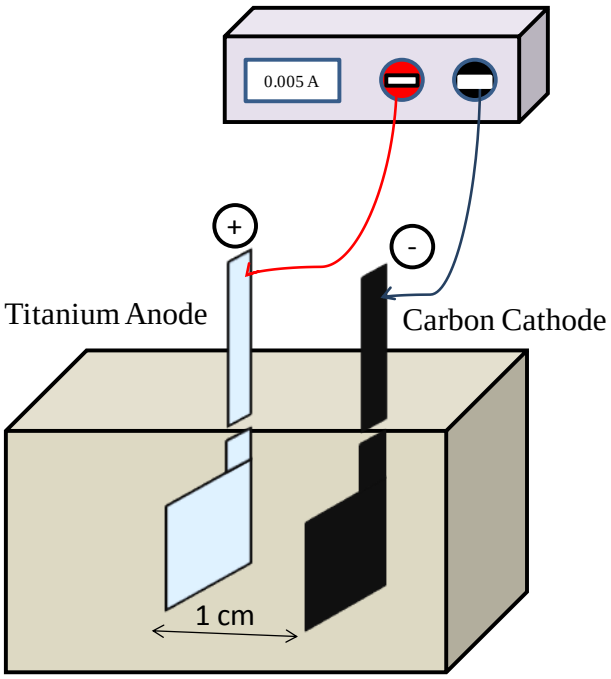

Figure 1. Schematic diagram for the electrochemical cell for anodic deposition of Ba/PbO_2 electrode

2.3 Analysis

The surface composition of as prepared Ba/PbO_2 electrode was analyzed by XRD patterns were obtained from a X'PERT-PRO X-ray diffractometer with Cu Ka radiation (λ=1.540598 Å)**.** The morphology of the Ba/PbO_2 samples was observed by SEM (Zeiss EVO-MA10). Solution phase ammonia oxidation analysis was performed by FTIR from Thermo scientific Nicolet iS5. The cyclic voltammetry measurements were performed using standard three electrode system connected to the computer control Potentiostat/Galvanostat model Versa STAT 3 from Princeton applied Research. As prepared $Ti/Ba/PbO_2$ was used as working electrode, platinum plate and an Ag/AgCl were used as counter and reference electrodes, respectively.

3. RESULTS AND DISCUSSION

3.1 Surface and interface characterization of Ba/PbO_2

Fig. 2 shows the SEM image of blank PbO_2 and the $Ba_{10\text{-}1}/PbO_2$ electrode. A cauliflower like morphology with 13 nm in size (see insert figure), as speculated in Fig. 2a. The uniformity may be due to the use of boric acid medium, which has a tendency to maintain pH that will facilitate to inhibit $Pb(OH)_2$ intermediate formation, which passivate the electrode and inhibit the nucleation and growth of lead dioxide [30].

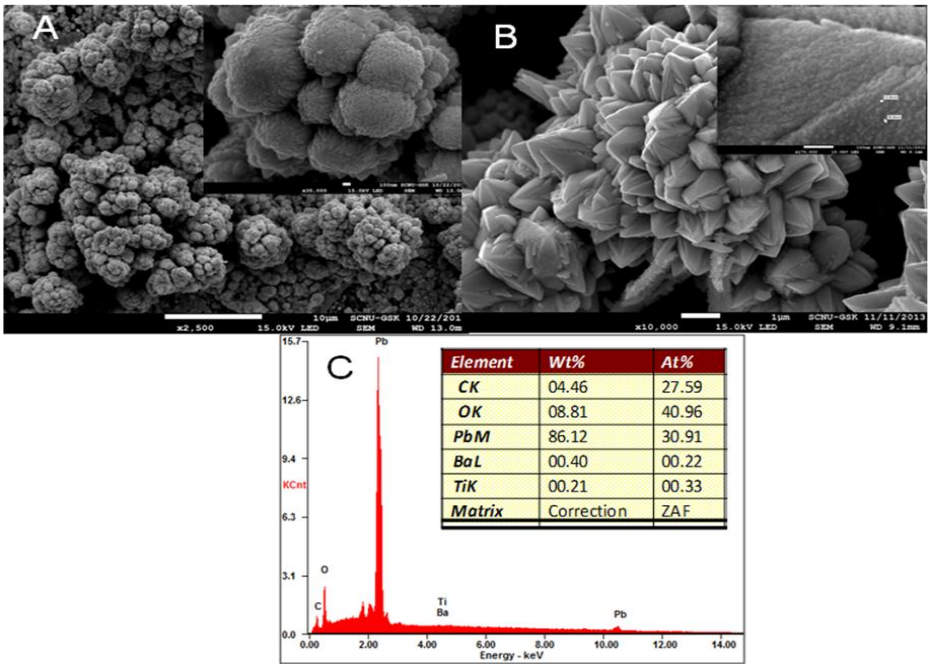

Figure 2. SEM images (A) PbO_2, (B) Barium doped PbO_2, (C) SEM-EDAX data for (B)

Fig. 2b. Shows SEM image of $Ba_{10\text{-}1}/PbO_2$ electrode, seems to be sharp edge like flower with all the wings of PbO_2 was connected towards the center point and radially arranged like sunflower. The

Insert figure shows that tiny particles with 15 nm in size on the each leaf like wings, which may be of Ba nano particles embedded on the PbO_2 surface.The presence of barium on the surface was confirmed by the Fig. 2c. SEM-EDAX with the atomic ratio of 0.22%. In the presence of barium, the PbO_2 morphology completely changed from cauliflower to a sharp edge like flower morphology that indicates barium ions influence. Similar, morphological surface is resulted in all ratios of Ba and PbO_2.

Fig. 3 depicts the XRD of PbO_2 and different ratios of Ba/PbO_2 electrodes. Fig. 3a.emphasizes the prepared electrode as β- PbO_2 that contains the phases of 110, 101 and 200 clearly correlated with reported work [31]. When Ba^{2+} ion introduced into the mixture, the PbO_2 phases changes depending upon the Ba ion concentration. The 0.6:1 concentration ratio of Ba to Pb ion shows $BaTiO_3$ (2θ values at ~ 28, 32 and 55) formation along with PbO_2 but its phase intensities have reduced and become amorphous. Further decreasing concentration of Ba ion the crystalinity of PbO_2 increased with absence of Ba ion in any form (Fig3 c-e). The peak intensity of PbO_2 at is maximum at a Ba ion concentration of 2 x 10^{-5} M (Fig. 3d) and the crystalinity retains, but barium peaks at 2θ value of 28° (111) [32] shows less intensity. In overall, high concentration of Ba ion makes more $BaTiO_3$ along with PbO_2 and lower concentrations makes more crystalline of PbO_2 upto 2 x 10^{-5} M less concentration of Ba ion enhanced the PbO_2 crystalinity, in other words more nano particles formed.

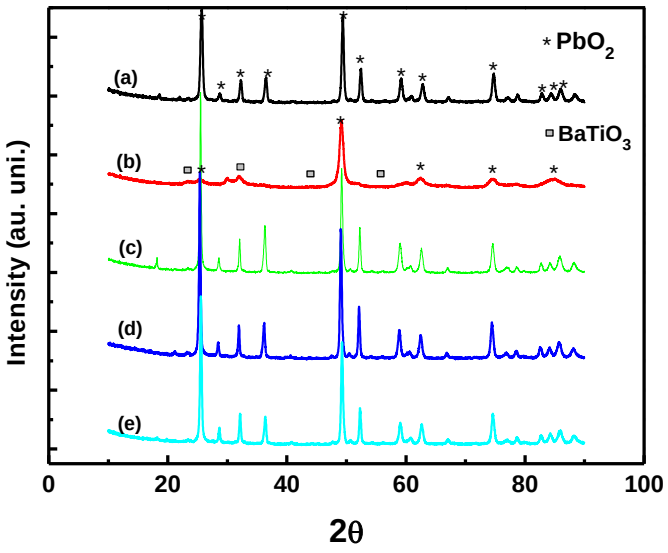

Figure 3. XRD images of Barium doped PbO_2 electrodes at different concentrations: (a) PbO_2; (b) $Ba_{10\text{-}1}/PbO_2$; (c) $Ba_{10\text{-}3}/PbO_2$; (d) $Ba_{10\text{-}5}/PbO_2$; (e) $Ba_{10\text{-}7}/PbO_2$.

Fig. 4 delineates the cyclic voltammetry response for the electrodeposited PbO_2 and Ba/PbO_2 electrodes in 0.1 M PBS (Phosphate buffer solution) solution. A characteristic PbO_2 peaks such as Pb^{2+} to Pb^{4+} oxidation was observed at 1.8 V in forward scan and the Pb^{4+} to Pb^{2+} reduction peak was observed nearly at 0.9 V in the reverse scan (Fig.4 insert). At the same time, the oxidation/reduction peak currents increased, between 400 µA to 14 mA, with decreasing concentration of Ba ion till 2 x 10^{-5} M (Fig.4 curves b-d). Further decreasing the Ba ion concentration, the oxidation/reduction peak current is started decreasing (Fig. 4e). The high peak current may be due to the higher surface area and

crystalinity of PbO_2 (Fig. 4d), which is well correlated with XRD results of 2 x 10^{-5} M of Ba ion (Fig.3d), where the phase intensity is higher and more crystalline of PbO_2 was observed. Therefore, the $Ba_{10\text{-}5}/PbO_2$ electrode was selected for further application.

Figure 4. Cyclic voltammetry response of PbO_2 and Ba/PbO_2 electrodes in 0.1M Phosphate buffer solution: (a) PbO_2; (b) $Ba_{10\text{-}1}/PbO_2$; (c) $Ba10_{\text{-}3}/PbO_2$; (d) $Ba_{10\text{-}5}/PbO_2$; (e) $Ba_{10\text{-}7}/PbO_2$. Scan rate= 20 mV/s.

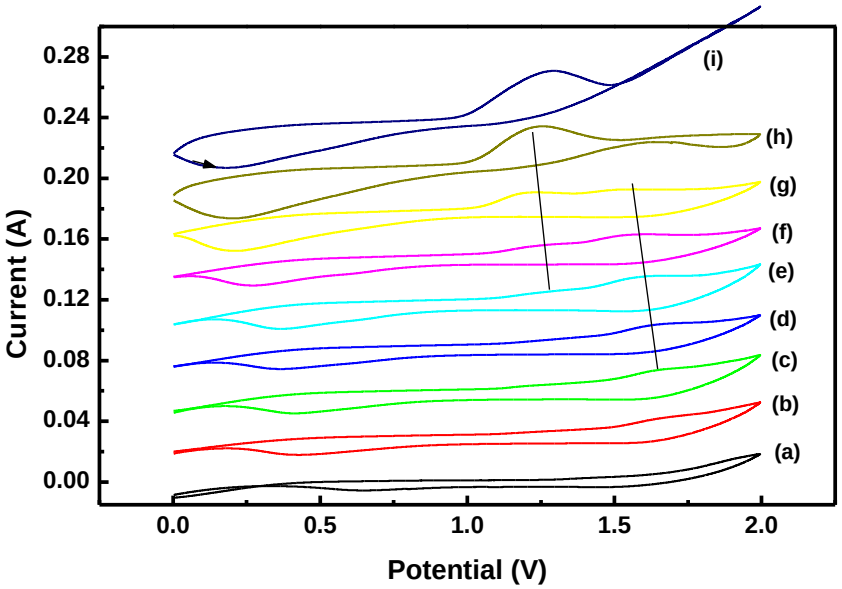

Figure 5. Cyclic voltammntry response of PbO_2 and $Ba_{10\text{-}5}/PbO_2$ electrodes in different pH adjusted with NaOH solution: (a) 6.5; (b) 7; (c) 9.4; (d) 10.8; (e) 11.35; (f) 12; (g) 12.35; (h) 12.7. Scan rate is 20 mV/s.

The effect of pH on the $Ba_{10\text{-}5}/PbO_2$ electrode was performed in 0.1M Na_2SO_4 solution at pH of 5.7 in the potential window corresponds to 0.0V to 2.0V (Fig.5 curve a). The pH of electrolyte slowly increased by the addition of the appropriate volume of NaOH and resulted CV are depicted in Fig.5b-i. At pH 5.7 the oxidation peak for Pb^{2+} to Pb^{4+} overlaid with oxygen evolution reaction and a reduction peak was existed at 0.66V in reverse scan. The oxidation peak potential is decreasing (move negative) with increasing the pH without an increase in peak current up to the pH of 11.4. There observes an addition hump like peak beyond pH 7, which corresponds to the PbO formation from Pb^{2+} ion. Similarly the reduction peak just moved towards less positive potential of 0.37 V with increasing the pH. But at pH 11.4 there observed direct oxidation of Pb^{2+} to Pb^{4+} (1.2 V) without an PbO intermediate peak and the reduction peak currents increased with shift in negative peak potential. At pH 12.3 there appears a single peak at 1.2 V that is responsible for α-PbO_2 with a steep raise in current that is responsible for oxygen evolution. A slightly basic medium shows one oxidation peak and which is more optimum to apply oxidation applications.

3.2 Catalytic oxidation of NH_3

Fig. 6 depicts the electro catalytic oxidation of NH_4OH on the $Ba_{10\text{-}5}/PbO_2$ electrode in the 0.01M NaOH solution. There found an oxidation peak at 1.17 V and a reduction peak at 0.27 V in the forward and reverse scan respectively (Fig.6A curve a). The oxidation peak may be related with the PbO_3^{2-} to PbO_2 and vice versa during reduction [25].

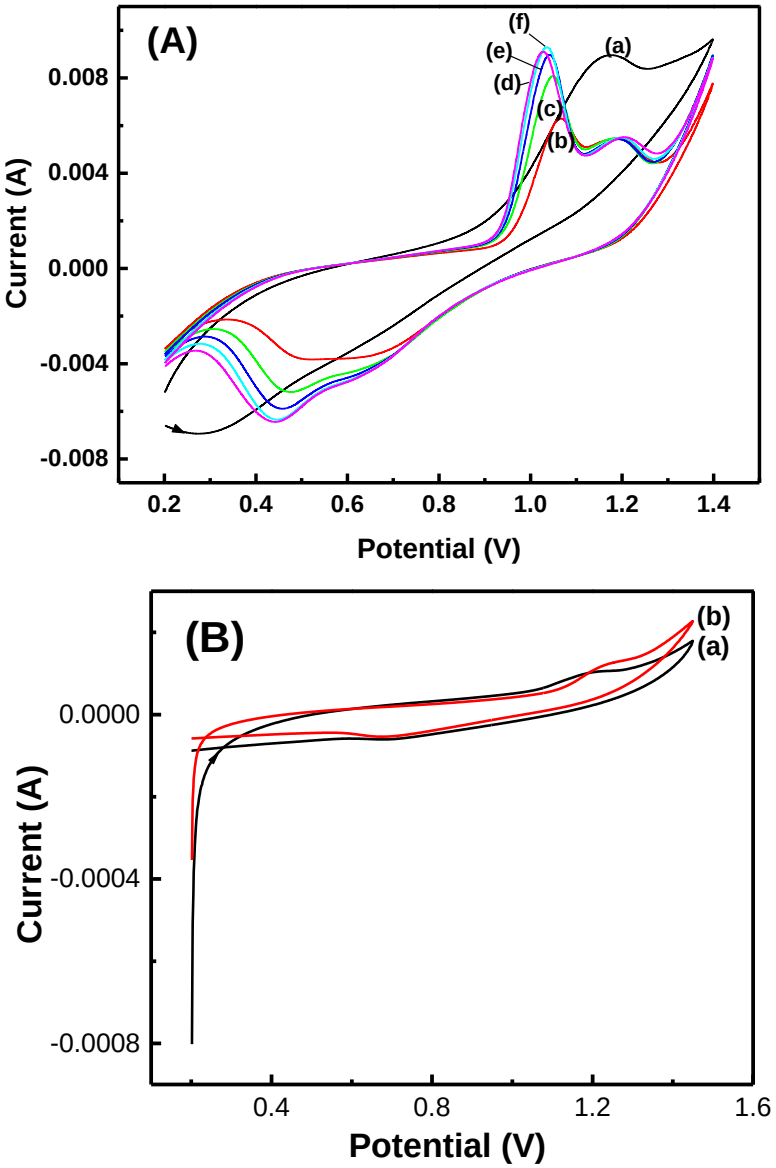

Figure 6 (A). Electrochemical oxidations of NH_4OH in 0.01M NaOH solution at $Ba_{10\text{-}5}/PbO_2$ electrode in 0.01 M NaOH solution with different concentration of NH_4OH: (a) without NH_3; (b) 1 mM; (c) 2.5 mM; (d) 5 mM; ® 10 mM; (f) 20 mM. Scan rate is 10 mV/s. **(B).** Electrochemical oxidation of only PbO_2 electrode (a) and (b) in presence of 20 mM NH_4OH in 0.1 M NaOH solution at scan rate of 10 mV s^{-1}.

Also this is confirmed by no curve crossing between the forward and reverse scan, where Pb^{2+} to PbO_2 formation [33]. In presence of 1 mM NH_4OH, an oxidation peak exists at 1.06 V along with

PbO_2 oxidation peak at 1.2 V. The pre-peak may be due to the oxidation of NH_3 by adsorption on electrode surface and adduct formation between NH_3 and PbO_3^{2-}, which is typical of CE mechanism (chemical reaction proceeded electron transfer reaction). The new two reduction peaks at 0.63V and 0.5 V in presence of NH_3, which is related to PbO_2 to Pb_3O_4 and PbO_2 to Pb^{2+} [33], concludes chemical reaction formation and formed Pb^{2+} during addition of NH_3. Note worth here that NH_3 oxidation has occurred at similar potential on BDD electrode [34]. But, only PbO_2 electrode shows no such oxidation of NH_3 (Fig.6B curve b) confirms the Ba influence in NH_3 oxidation. The pre-peak current increases with increasing concentration of NH_3 (Fig. 6A curve c-f) and saturated at 20 mM NH_3, which evidences the oxidation relationship between Pb^{2+} and NH_3 with influence of Ba.

Further, the bulk electrolysis done at $Ba_{10\text{-}5}/PbO_2$ electrode in the presence of 20 mM of NH_4OH in 60 Sec and that sample analyzed through FT-IR. The obtained results are presented in Fig. 7. There appears N-H stretching frequency peak at 1043 cm^{-1} wave numbers in before electrolysis. After electrolysis, the N-H stretching peak complexly absent. Also, there is a huge increase in N-O symmetry stretching peak at ~1643 cm^{-1} wave numbers clearly indicate NH_3 oxidation and formation of NO_x compounds [35]. It is known that metal oxide in base medium follows the similar mechanistic pathway [36] as shown in equations 1 and 2.

$$NH_3 + 7OH^- \longrightarrow NO_2^- + 5H_2O + 6e \quad \text{---(1)}$$

$$NH_3 + 9OH^- \longrightarrow NO_3^- + 6H_2O + 8e \quad \text{---(2)}$$

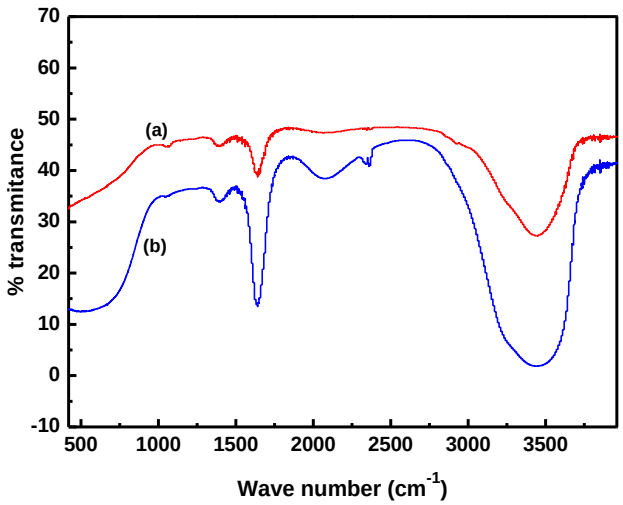

Figure 7. FT-IR spectra of initial (a) and 60 Sec electrolyzed (b) samples of 20 mM NH_4OH in 0.01 M NaOH solution. Conditions: Fixed potential = 1 V (Ag/AgCl); Electrode = $Ba_{10\text{-}5}/PbO_2$ with 1 cm^2.

4. CONCLUSIONS

The nano structured Ba doped PbO_2 was electrochemically fabricated on Ti electrode with the optimized barium concentration. Barium ion addition confirms by morphological change from Cauliflower structure sharp edge like flower structure. Low concentration of barium ion addition ($Ba_{10\text{-}}$

$_5$/PbO_2) demonstrates nano crystallinity of PbO_2, which is confirmed by XRD and cyclic voltammetry. Further, nano structured $Ba_{10\text{-}5}$/PbO_2 electrode effectively oxidizes NH_3 at low potential in the NaOH solution. The results are promising and can be enhanced to real applications.

ACKNOWLEDGEMENT
This work was supported by the National Research Foundation of Korea (NRF) funded by the Korea government (MEST) (Grant No. 2014001974).

Reference

1. N. Thuc Phan, K. Hyun Kim, Z. Ho Shon, E. Chan Jeon, K. Jung and N. Jin Kim, *Atmos. Environ,* 65 (2013) 177-185.
2. M. Vidotti, L.H. Dall, S.I. Cordoba de Torresi, K. Bergamaski and F.C. Nart, *Anal. Chim. Acta,* 489 (2003) 207-214.
3. B.A. Lopez de Mishima, D. Lescano,T. Molina Holgado and H.T. Mishima, *Electrochim. Acta*, 43: 395-404.
4. A.C.A. De Vooys, M.T.M. Koper, R.A. Van Santen, and J.A.R. Van Veen, *J. Electroanal.Chem.,* 506 (2001) 127-137.
5. D. Giovanelli, M.C. Buzzeo, N.S. Lawrence, C. Hardacre, K.R. Seddon and R.G. Compton, *Talanta,* 62 (2004) 904- 911.
6. I. Suárez,G. Bodega and B. Fernández, *Neuro.Chem.Int.,* 41 (2002) 123-142.
7. D. Dirtu, L. Odochian, A. Pui, and I. Humelnicu, *Cent. Eur. J. Chem.,* 4 (2006) 666-673.
8. A.H.White and Wm.Melville, *J. Am. Chem. Soc., 27 (1905)* 373–386.
9. A.A. Konnov and J. De. Ruyck, *Combust.Sci.and Tech.,* 152 (2000) 23-37.
10. A. Kapałkaa, S. Fierro, Z. Frontistis, A. Katsaounis, S. Neodo, O. Frey, N.de. Rooij, K.M.Udert and C.Comninellis, *Electro.Chim.Acta.,* 56 (2011) 1361–1365.
11. S. Heylen, S. Smet, K.G.M. Laurier, J. Hofkens, M.B.J. Roeffaers and J.A. Martens, *Catal. Sci.Technol.,* 2 (2012) 1802–1805.
12. P.D. Sobczyk, E.J.M. Hensen, A.M.de. Jong and A.S.Van Santen, *Top.Catalysis*, 23 (2003) 109-117.
13. N.I Il'chenko, *Russ.Chem. Rev.,* 45 (1976) 1119-1134.
14. F. Shao, F.H. Ramirez, J.D. Prades, J.R. Morante and N. Lopez, *Proced. Eng,* 47 (2012) 293– 297.
15. R.Q. Long and R.T. Yang, *Chem.Comm.,* 17 (2000) 1651-1652.
16. S.J. Juutilainen, P.A. Simell and A.O.I. Krause, *Appl. Catal., B,* 62 (2006) 86–92.
17. H. Gerischer and A. Mauerer, *J. Electroanal. Chem.Interfac.Electrochem.,* 25 (1970) 421-433.
18. N.L. Michels, A. Kapałka, A.A. Abd-El-Latif , H. Baltruschat and C. Comninellis, *Electro.Commun.,* 12 (2010) 1199–1202.
19. T.L. Lomocso and E.A. Baranova, *Electrochim. Acta,* 56 (2011) 8551–8558.
20. Y. Wang, X. Guo, J. Li, Y. Yang, Z. Leiand Zhang, *Open J. Appl.*, 2 (2012) 241-247.
21. R. Cossu, A.M. Polcaro, M.C. Lavagnolo, M. Mascia, S. Palmas and F. Renoldi, *Environ. Sci.Technol.*, 32 (1998) 3570-3573.
22. X. Ma, R. Wang, W. Guo, H. Yang, Z. Liang and C. Fan, *Int.J. Electrochem. Sci.,* 7 (2012)6012-6024.
23. Y.H. Song and L. Jie Ma, *Advan.Mater. Res.*, 743 (2013) 218-222.
24. A. Fernandes, D. Santos, M.J. Pacheco, and L. Ciríaco and A. Lopes, *Appl.Catal. B,* 148–149 (2014) 288–294.
25. B. Sljukic, C.E. Banks, A. Crossley and R.G. Compton, *Anal.Chim. Acta,* 587 (2007) 240–246.
26. J.M. Tulliani, C. Baroni, C. Lopez and L. Dessemond, *J.Eur.Ceram.Soc*, 31 (2011) 2357– 2364.

27. P. Vernoux and X. Li, *Appl.Catal. B,* 61 (2005) 267–273.
28. H. Karami and A. Yaghoobi, *J. Clust.Sci,* 21 (2010) 725–737.
29. C. Hamel, T. Brousse, D.B. Elanger and D. Guaya, *J. Electrochemical Soc,* 159 (2012) A60-A67.
30. K. De Wael, M. De Keersmaecker, M. Dowsett, D. Walker, P.A. Thomas, and A. Adriaens,*J.Solid State Electrochem*, 14 (2010) 407-413.
31. Z. Chen, Q.Yu, D. Hui Liao, Z. Cheng Guo and J. Wu , *Trans. Nonferrous Met.Soc.China*, 23(2013) 1382−1389.
32. V.F. Solovyov, H.J. Wiesmann and M. Suenaga, *Supercond. Sci.Technology*, 16 (2003) L37-L3.
33. S. He, R. Xu, S. Han, J. Wang, B. Chen, *J. Electrochem. Soc.*, 163 (2016) D265-D270.
34. X. Ji, C.E. Banks and R.G. Compton, *Analyst*, 130 (2005) 1345–1347.
35. J. Coates. *Interpretation of Infrared Spectra, A Practical Approach*, R.A. Meyers (Ed.) John Wiley & Sons Ltd, Chichester (2000) 10815–10837.
36. N.J. Bunce and D. Bejan, *Electrochim. Acta,* 56 (2011) 8085 – 8093.